

Pion-induced production of $\Lambda(1520)$ hyperons on nuclei near threshold

E. Ya. Paryev^{1,2}, Yu. T. Kiselev²

¹*Institute for Nuclear Research, Russian Academy of Sciences,
Moscow 117312, Russia*

²*Institute for Theoretical and Experimental Physics,
Moscow 117218, Russia*

Abstract

We study the pion-induced inclusive $\Lambda(1520)$ hyperon production from nuclei near threshold within a nuclear spectral function approach accounting for incoherent primary π^- meson-proton $\pi^- p \rightarrow K^0 \Lambda(1520)$ production processes. We calculate the absolute differential and total cross sections for the production of $\Lambda(1520)$ hyperons off carbon and tungsten nuclei at laboratory angles of $0^\circ-10^\circ$, $10^\circ-45^\circ$ and $45^\circ-85^\circ$ by π^- mesons with momentum of 1.7 GeV/c as well as their relative (transparency ratio) differential and integral yields from these nuclei within four scenarios for their total in-medium width. We demonstrate that these absolute observables, contrary to the relative ones, reveal some sensitivity to the $\Lambda(1520)$ in-medium width. Therefore, their measurement in a dedicated experiment at the GSI pion beam facility will allow to shed light on this width.

1 Introduction

The study of the renormalization of the properties, masses and widths, of light vector mesons ρ , ω , ϕ , kaons and antikaons, η , η' and J/ψ mesons in nuclei has received considerable interest in recent years (see, for example, [1–9]). The in-medium properties of hyperons at finite density have also become a topic of intense current theoretical investigations [10–16]. Thus, for instance, the medium modifications of $\Sigma(1385)$ and $\Lambda(1520)$ hyperons have been studied within chiral unitary hadronic theory [10, 11]. Very small mass shifts of about -40 and -20 MeV have been predicted for the $\Sigma(1385)$ and $\Lambda(1520)$ hyperons, respectively, at rest at normal nuclear matter density ρ_0 . Moreover, a moderate increase of the width of $\Sigma(1385)$ by the factor ~ 2 –3 at density ρ_0 compared to the free width ~ 35 MeV and appreciable increase of the width of $\Lambda(1520)$ hyperons at this density by the factor ~ 5 with respect to the free width of 15.6 MeV has been calculated. The influence of the $\Lambda(1520)$ hyperon in-medium width on its yield from pA and γA reactions has been analyzed within collisional models [17–19] using an eikonal approximation. It has been shown that both the momentum dependence of the absolute $\Lambda(1520)$ hyperon yield and the A dependence of its relative yield are quite sensitive to the $\Lambda(1520)$ in-medium width.

Valuable information on the in-medium properties of $\Lambda(1520)$ hyperons, complementary to that from proton–nucleus and photon–nucleus collisions, can be inferred from pion–nucleus reactions. In this context, the main aim of the present study is to give the predictions for the absolute differential and total cross sections for production of $\Lambda(1520)$ hyperons in $\pi^{-12}\text{C} \rightarrow \Lambda(1520)X$ and $\pi^{-184}\text{W} \rightarrow \Lambda(1520)X$ reactions at 1.7 GeV/c incident pion momentum as well as for their relative (transparency ratio) differential and integral yields from these reactions within different scenarios for $\Lambda(1520)$ total in-medium width. These nuclear targets and this initial beam momentum were adopted in recent measurements [20] of π^- meson-induced ϕ meson production at the GSI pion beam facility using the HADES spectrometer and, therefore, can be employed in studying the $\pi^- A \rightarrow \Lambda(1520)X$ interactions here. The calculations are based on a first-collision model, developed in [21] for the analysis of the inclusive ϕ meson production data [20] and extended to account for different scenarios for the $\Lambda(1520)$ in-medium width. These calculations can be used as an important tool for determining the width from the data which could be taken in a dedicated experiment at the GSI pion beam facility.

2 Direct $\Lambda(1520)$ hyperon production mechanism

The $\Lambda(1520)$ hyperons can be produced directly in $\pi^- A$ ($A = {}^{12}\text{C}$ and ${}^{184}\text{W}$) reactions at incident momentum of 1.7 GeV/c in the following $\pi^- p$ elementary process with the lowest free production threshold momentum (1.68 GeV/c) ¹⁾

$$\pi^- + p \rightarrow K^0 + \Lambda(1520). \quad (1)$$

Taking into consideration that the in-medium threshold energy ²⁾ of the process (1) looks like that for the free final particles due to the cancelation of nuclear scalar potentials $U_{K^0} \approx +20$ MeV [5] and $U_{\Lambda(1520)} \approx -20$ MeV [10], felt by the K^0 mesons and low-momentum $\Lambda(1520)$ hyperons at saturation density ρ_0 , as well as for the reason of reducing the possible uncertainty of our calculations due to use in them of the model $\Lambda(1520)$ self-energy [10] at finite momenta studied in the present work, we will ignore here the medium modification of the outgoing hadron masses at these momenta.

¹⁾ We can neglect the processes $\pi^- N \rightarrow K\Lambda(1520)\pi$ with one pion in the final state at the incident pion momentum of 1.7 GeV/c, because they are energetically suppressed due to the fact that this momentum is less than their production threshold momentum of 1.98 GeV/c in vacuum $\pi^- N$ collisions. Moreover, taking into account the results of the study [21] of pion-induced ϕ meson production on ${}^{12}\text{C}$ and ${}^{184}\text{W}$ nuclei at beam momentum of 1.7 GeV/c, we ignore in the present work by analogy with [21] the secondary pion–nucleon $\pi N \rightarrow K\Lambda(1520)$ production processes.

²⁾ Determining the strength of the $\Lambda(1520)$ production cross sections in $\pi^- A$ collisions near threshold (cf. [21]).

Since the $\Lambda(1520)$ -nucleon elastic cross section is expected to be small similar to the ΛN elastic cross section at these momenta [22], we will neglect quasielastic $\Lambda(1520)N$ rescatterings in the present study. Then, accounting for the absorption of the incident pion and $\Lambda(1520)$ hyperon in nuclear matter as well as using the results given in [21], we represent the inclusive differential cross section for the production of $\Lambda(1520)$ hyperons with vacuum momentum $\mathbf{p}_{\Lambda(1520)}$ (or \mathbf{p}_{Λ^*}) on nuclei in the direct process (1) as follows:

$$\frac{d\sigma_{\pi^- A \rightarrow \Lambda(1520)X}^{(\text{prim})}(\mathbf{p}_{\pi^-}, \mathbf{p}_{\Lambda^*})}{d\mathbf{p}_{\Lambda^*}} = I_V[A, \theta_{\Lambda^*}] \left(\frac{Z}{A} \right) \left\langle \frac{d\sigma_{\pi^- p \rightarrow K^0 \Lambda(1520)}(\mathbf{p}_{\pi^-}, \mathbf{p}_{\Lambda^*})}{d\mathbf{p}_{\Lambda^*}} \right\rangle_A, \quad (2)$$

where

$$I_V[A, \theta_{\Lambda^*}] = A \int_0^R r_{\perp} dr_{\perp} \int_{-\sqrt{R^2 - r_{\perp}^2}}^{\sqrt{R^2 - r_{\perp}^2}} dz \rho(\sqrt{r_{\perp}^2 + z^2}) \exp \left[-\sigma_{\pi^- N}^{\text{tot}} A \int_{-\sqrt{R^2 - r_{\perp}^2}}^z \rho(\sqrt{r_{\perp}^2 + x^2}) dx \right] \quad (3)$$

$$\times \int_0^{2\pi} d\varphi \exp \left[- \int_0^{l(\theta_{\Lambda^*}, \varphi)} \frac{dx}{\lambda_{\Lambda^*}(\sqrt{x^2 + 2a(\theta_{\Lambda^*}, \varphi)x + b + R^2})} \right], \quad (4)$$

$$a(\theta_{\Lambda^*}, \varphi) = z \cos \theta_{\Lambda^*} + r_{\perp} \sin \theta_{\Lambda^*} \cos \varphi, \quad b = r_{\perp}^2 + z^2 - R^2, \quad (4)$$

$$l(\theta_{\Lambda^*}, \varphi) = \sqrt{a^2(\theta_{\Lambda^*}, \varphi) - b - a(\theta_{\Lambda^*}, \varphi)}, \quad (5)$$

$$\lambda_{\Lambda^*}(|\mathbf{r}|) = \frac{p_{\Lambda^*}}{M_{\Lambda^*} \Gamma_{\Lambda^*}(|\mathbf{r}|)} \quad (6)$$

and

$$\left\langle \frac{d\sigma_{\pi^- p \rightarrow K^0 \Lambda(1520)}(\mathbf{p}_{\pi^-}, \mathbf{p}_{\Lambda^*})}{d\mathbf{p}_{\Lambda^*}} \right\rangle_A = \int \int P_A(\mathbf{p}_t, E) d\mathbf{p}_t dE \quad (7)$$

$$\times \left\{ \frac{d\sigma_{\pi^- p \rightarrow K^0 \Lambda(1520)}[\sqrt{s}, M_{\Lambda^*}, m_{K^0}, \mathbf{p}_{\Lambda^*}]}{d\mathbf{p}_{\Lambda^*}} \right\}, \quad (8)$$

$$s = (E_{\pi^-} + E_t)^2 - (\mathbf{p}_{\pi^-} + \mathbf{p}_t)^2, \quad (8)$$

$$E_t = M_A - \sqrt{(-\mathbf{p}_t)^2 + (M_A - m_N + E)^2}. \quad (9)$$

Here, $d\sigma_{\pi^- p \rightarrow K^0 \Lambda(1520)}[\sqrt{s}, M_{\Lambda^*}, m_{K^0}, \mathbf{p}_{\Lambda^*}]/d\mathbf{p}_{\Lambda^*}$ is the off-shell inclusive differential cross section for the production of $\Lambda(1520)$ hyperon and K^0 meson with free masses M_{Λ^*} and m_{K^0} , respectively. The $\Lambda(1520)$ hyperon is produced with vacuum momentum \mathbf{p}_{Λ^*} in reaction (1) at the $\pi^- p$ center-of-mass energy \sqrt{s} . E_{π^-} and \mathbf{p}_{π^-} are the total energy and momentum of the incident pion ($E_{\pi^-} = \sqrt{m_{\pi}^2 + \mathbf{p}_{\pi^-}^2}$, m_{π} is the free space pion mass); $\rho(\mathbf{r})$ and $P_A(\mathbf{p}_t, E)$ are the local nucleon density and the spectral function of the target nucleus A normalized to unity; \mathbf{p}_t and E are the internal momentum and removal energy of the struck target proton involved in the collision process (1); $\sigma_{\pi^- N}^{\text{tot}}$ is the total cross section of the free $\pi^- N$ interaction (we use in our calculations the value of $\sigma_{\pi^- N}^{\text{tot}} = 35$ mb for initial pion momentum of 1.7 GeV/c [21]); $\Gamma_{\Lambda^*}(|\mathbf{r}|)$ is the total $\Lambda(1520)$ width in its rest frame, taken at the point \mathbf{r} inside the nucleus and at the pole mass M_{Λ^*} ; Z and A are the numbers of protons and nucleons in the target nucleus, and M_A and R are its mass and radius; m_N is the free space nucleon mass; and θ_{Λ^*} is the polar angle of vacuum momentum \mathbf{p}_{Λ^*} in the laboratory system with z-axis directed along the momentum \mathbf{p}_{π^-} of the incoming pion beam.

For the nuclear density $\rho(\mathbf{r})$ of the ^{12}C and ^{184}W nuclei of interest, we have adopted, correspondingly, the harmonic oscillator and the Woods-Saxon distributions given in Ref. [21]. For these target nuclei, the nuclear spectral function $P_A(\mathbf{p}_t, E)$ was taken from Refs. [21, 23–25].

Following [21], we suppose that the off-shell differential cross section $d\sigma_{\pi^-p \rightarrow K^0\Lambda(1520)}[\sqrt{s}, M_{\Lambda^*}, m_{K^0}, \mathbf{p}_{\Lambda^*}]/d\mathbf{p}_{\Lambda^*}$ for $\Lambda(1520)$ production in process (1) is equivalent to the respective on-shell cross section calculated for the off-shell kinematics of this process as well as for the final $\Lambda(1520)$ and kaon free space masses M_{Λ^*} and m_{K^0} , respectively. Accounting for Eq. (14) from [21], we obtain the following expression for this cross section:

$$\begin{aligned} \frac{d\sigma_{\pi^-p \rightarrow K^0\Lambda(1520)}[\sqrt{s}, M_{\Lambda^*}, m_{K^0}, \mathbf{p}_{\Lambda^*}]}{d\mathbf{p}_{\Lambda^*}} &= \frac{\pi}{I_2[s, M_{\Lambda^*}, m_{K^0}]E_{\Lambda^*}} \\ &\times \frac{d\sigma_{\pi^-p \rightarrow K^0\Lambda(1520)}(\sqrt{s}, M_{\Lambda^*}, m_{K^0}, \theta_{\Lambda^*}^*)}{d\Omega_{\Lambda^*}^*} \\ &\times \frac{1}{(\omega + E_t)} \delta \left[\omega + E_t - \sqrt{m_{K^0}^2 + (\mathbf{Q} + \mathbf{p}_t)^2} \right], \end{aligned} \quad (10)$$

where

$$I_2[s, M_{\Lambda^*}, m_{K^0}] = \frac{\pi}{2} \frac{\lambda[s, M_{\Lambda^*}^2, m_{K^0}^2]}{s}, \quad (11)$$

$$\lambda(x, y, z) = \sqrt{[x - (\sqrt{y} + \sqrt{z})^2][x - (\sqrt{y} - \sqrt{z})^2]}, \quad (12)$$

$$\omega = E_{\pi^-} - E_{\Lambda^*}, \quad \mathbf{Q} = \mathbf{p}_{\pi^-} - \mathbf{p}_{\Lambda^*}, \quad E_{\Lambda^*} = \sqrt{M_{\Lambda^*}^2 + \mathbf{p}_{\Lambda^*}^2}. \quad (13)$$

Here, $d\sigma_{\pi^-p \rightarrow K^0\Lambda(1520)}(\sqrt{s}, M_{\Lambda^*}, m_{K^0}, \theta_{\Lambda^*}^*)/d\Omega_{\Lambda^*}^*$ is the off-shell differential cross section for the production of $\Lambda(1520)$ hyperons in reaction (1) under the polar angle $\theta_{\Lambda^*}^*$ in the π^-p c.m.s. This cross section is assumed to be isotropic in our model calculations of $\Lambda(1520)$ hyperon production in pion–nucleus interactions:

$$\frac{d\sigma_{\pi^-p \rightarrow K^0\Lambda(1520)}(\sqrt{s}, M_{\Lambda^*}, m_{K^0}, \theta_{\Lambda^*}^*)}{d\Omega_{\Lambda^*}^*} = \frac{\sigma_{\pi^-p \rightarrow K^0\Lambda(1520)}(\sqrt{s}, \sqrt{s_{\text{th}}})}{4\pi}. \quad (14)$$

Here, $\sigma_{\pi^-p \rightarrow K^0\Lambda(1520)}(\sqrt{s}, \sqrt{s_{\text{th}}})$ is the "in-medium" total cross section of reaction (1) having the threshold energy $\sqrt{s_{\text{th}}} = M_{\Lambda^*} + m_{K^0} = 2.017$ GeV. According to the aforesaid, it is equivalent to the vacuum cross section $\sigma_{\pi^-p \rightarrow K^0\Lambda(1520)}(\sqrt{s}, \sqrt{s_{\text{th}}})$, in which the free collision energy $s = (E_{\pi^-} + m_N)^2 - \mathbf{p}_{\pi^-}^2$ is replaced by the in-medium expression (8). For the vacuum total cross section $\sigma_{\pi^-p \rightarrow K^0\Lambda(1520)}(\sqrt{s}, \sqrt{s_{\text{th}}})$ we have employed the following parametrization suggested in Ref. [19]:

$$\sigma_{\pi^-p \rightarrow K^0\Lambda(1520)}(\sqrt{s}, \sqrt{s_{\text{th}}}) = \begin{cases} 123 (\sqrt{s} - \sqrt{s_{\text{th}}})^{0.47} [\mu\text{b}] & \text{for } 0 < \sqrt{s} - \sqrt{s_{\text{th}}} \leq 0.427 \text{ GeV}, \\ 26.6 / (\sqrt{s} - \sqrt{s_{\text{th}}})^{1.33} [\mu\text{b}] & \text{for } \sqrt{s} - \sqrt{s_{\text{th}}} > 0.427 \text{ GeV}. \end{cases} \quad (15)$$

As seen from Fig. 1, the parametrization (15) (solid line) fits well the existing set of experimental data (full circles) [26] for the $\pi^-p \rightarrow K^0\Lambda(1520)$ reaction. One can also see that the on-shell cross section $\sigma_{\pi^-p \rightarrow K^0\Lambda(1520)}$ amounts approximately to $13 \mu\text{b}$ for the initial pion momentum of 1.7 GeV/c and a free target proton being at rest. The off-shell cross section $\sigma_{\pi^-p \rightarrow K^0\Lambda(1520)}$, calculated in line with Eqs. (8), (9), (15) for a pion momentum of 1.7 GeV/c and a target proton bound in ^{12}C by 16 MeV and having relevant internal momentum of 250 MeV/c, is about $53 \mu\text{b}$. This offers the possibility of measuring the $\Lambda(1520)$ yield in π^-A reactions at the very near-threshold beam momentum of 1.7 GeV/c at the GSI pion beam facility with sizeable strength.

Accounting for the HADES spectrometer acceptance, we will consider the $\Lambda(1520)$ momentum distributions on ^{12}C and ^{184}W target nuclei in three laboratory solid angles $\Delta\Omega_{\Lambda^*}=0^\circ \leq \theta_{\Lambda^*} \leq 10^\circ$, $10^\circ \leq \theta_{\Lambda^*} \leq 45^\circ$, $45^\circ \leq \theta_{\Lambda^*} \leq 85^\circ$ and $0 \leq \varphi_{\Lambda^*} \leq 2\pi$. Here, φ_{Λ^*} is the azimuthal angle of the

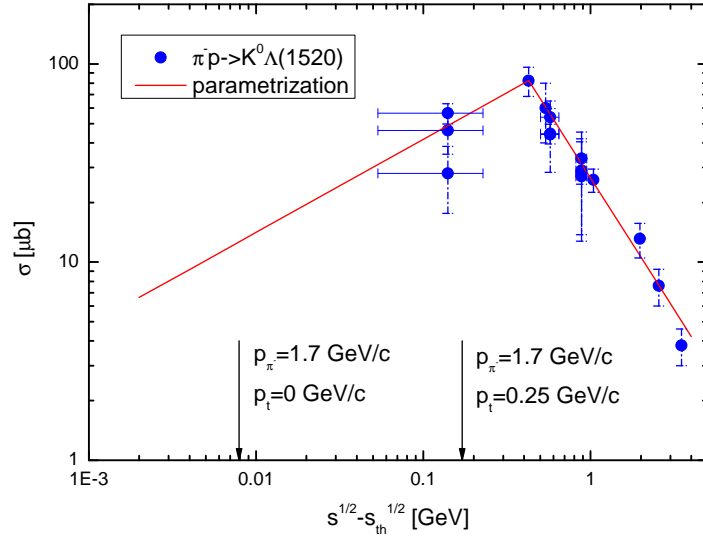


Figure 1: (color online) Total cross section for the reaction $\pi^- p \rightarrow K^0 \Lambda(1520)$ as a function of the excess energy $\sqrt{s} - \sqrt{s_{\text{th}}}$. The left and right arrows indicate the excess energies $\sqrt{s} - \sqrt{s_{\text{th}}} = 7.9$ MeV and $\sqrt{s} - \sqrt{s_{\text{th}}} = 171$ MeV corresponding to the incident pion momentum of $|\mathbf{p}_{\pi^-}| = 1.7$ GeV/c and a free target proton at rest and a target proton bound in ^{12}C by 16 MeV and having momentum of 250 MeV/c directed opposite to the incoming pion beam. For the rest of notation see text.

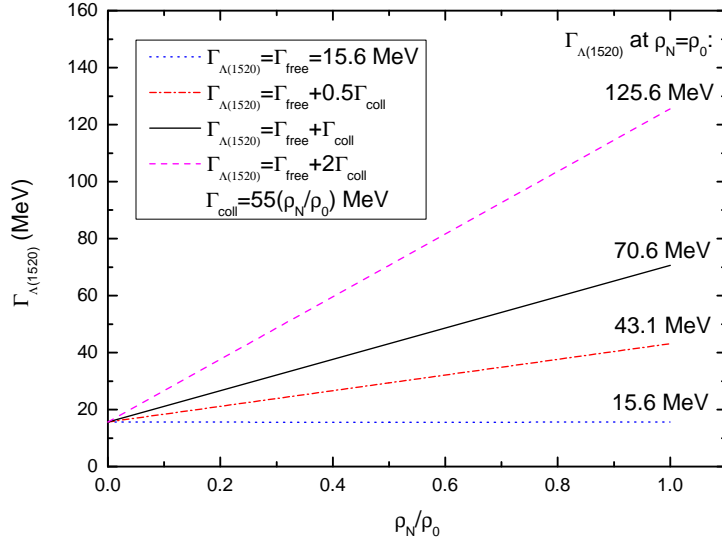


Figure 2: (color online) $\Lambda(1520)$ hyperon total width in its rest frame as a function of the density. For notation see text.

$\Lambda(1520)$ momentum \mathbf{p}_{Λ^*} in the laboratory system. Integrating the full inclusive differential cross section (2) over these ranges, we can represent the differential cross section for $\Lambda(1520)$ hyperon production in $\pi^- A$ collisions from the direct process (1), corresponding to the HADES acceptance

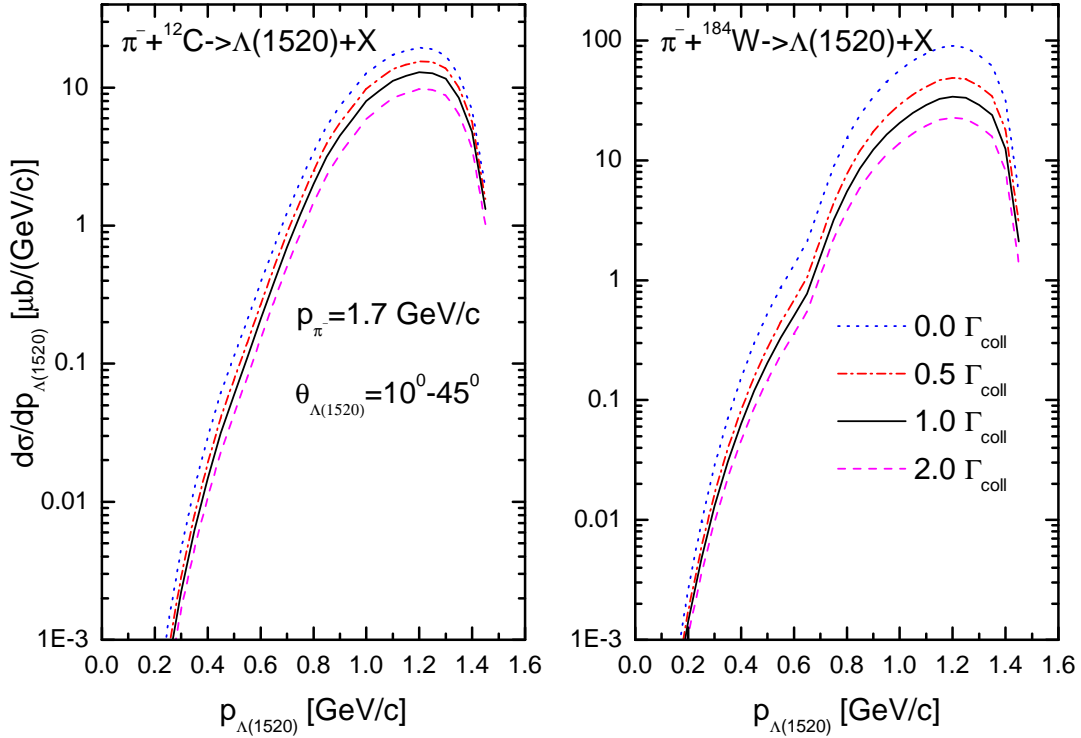


Figure 3: (color online) Momentum differential cross sections for the production of $\Lambda(1520)$ hyperons from the primary $\pi^- p \rightarrow K^0 \Lambda(1520) + X$ channel in the laboratory polar angular range of 10° – 45° in the interaction of π^- mesons of momentum of 1.7 GeV/c with ^{12}C (left) and ^{184}W (right) nuclei, calculated within different scenarios for the total $\Lambda(1520)$ hyperon in-medium width in which its collisional width was multiplied by the factors indicated in the inset.

window ³⁾, in the following form:

$$\begin{aligned} \frac{d\sigma_{\pi^- A \rightarrow \Lambda(1520)X}^{(\text{prim})}}{dp_{\Lambda^*}} &= \int_{\Delta\Omega_{\Lambda^*}} d\Omega_{\Lambda^*} \frac{d\sigma_{\pi^- A \rightarrow \Lambda(1520)X}^{(\text{prim})}(\mathbf{p}_{\pi^-}, \mathbf{p}_{\Lambda^*})}{d\mathbf{p}_{\Lambda^*}} p_{\Lambda^*}^2 \\ &= 2\pi \left(\frac{Z}{A}\right) \int_a^b d\cos\theta_{\Lambda^*} I_V[A, \theta_{\Lambda^*}] \left\langle \frac{d\sigma_{\pi^- p \rightarrow K^0 \Lambda(1520)}(p_{\pi^-}, p_{\Lambda^*}, \theta_{\Lambda^*})}{dp_{\Lambda^*} d\Omega_{\Lambda^*}} \right\rangle_A, \end{aligned} \quad (16)$$

where $(a, b) = (\cos 10^\circ, 1), (\cos 45^\circ, \cos 10^\circ)$ and $(\cos 85^\circ, \cos 45^\circ)$.

We define now the $\Lambda(1520)$ total in-medium width appearing in Eq. (6) and used in our calculations of $\Lambda(1520)$ production in $\pi^- A$ reactions. For this width, we employ two different scenarios [19]: i) no in-medium effects and, correspondingly, the scenario with the free $\Lambda(1520)$ width (dotted line in Fig. 2); ii) the sum of the free $\Lambda(1520)$ width and its collisional width Γ_{coll} of the type [10, 11, 17] $55(\rho_N/\rho_0)$ MeV, where ρ_N is the total nucleon density (solid line ⁴⁾ in Fig. 2). In order to study the sensitivity of the $\Lambda(1520)$ hyperon production cross sections from the channel (1) to its total in-medium width we will also adopt in our calculations yet two additional scenarios for this

³⁾ At HADES the $\Lambda(1520)$ hyperons could be identified via the decays $\Lambda(1520) \rightarrow K^- p$ with a branching ratio of 22.5%.

⁴⁾ In this scenario the resulting total width of the $\Lambda(1520)$ hyperon reaches the value of about 70 MeV at the normal nuclear matter density ρ_0 , which is a factor of ~ 5 larger than the free one.

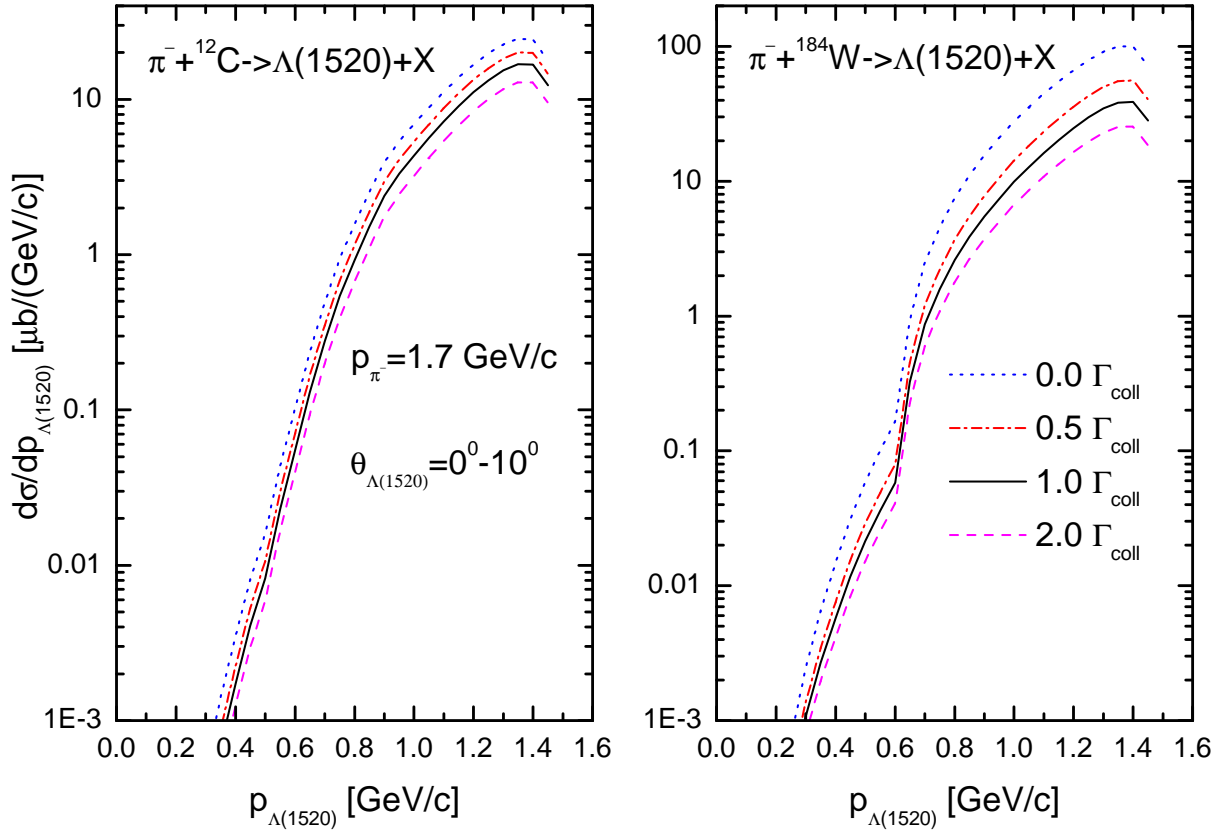


Figure 4: (color online) The same as in Fig.3 but for the laboratory polar angular range of $0^\circ-10^\circ$.

width, in which, as compared to the scenario ii), the $\Lambda(1520)$ nominal collisional width Γ_{coll} defined above was artificially multiplied by factors $f = 0.5$ and $f = 2$ [17] (dotted-dashed and dashed lines in Fig. 2)⁵⁾.

The $\Lambda(1520)$ in-medium width can be extracted from a comparison of the calculated (see Eq. (16)) and measured momentum distributions on ^{12}C and ^{184}W target nuclei. Additionally, valuable information concerning the $\Lambda(1520)$ absorption in nuclear matter can be obtained [17, 19] from a comparison of the calculations with the measured transparency ratio of the $\Lambda(1520)$ hyperon, normalized to carbon:

$$T_A = \frac{12 \sigma_{\Lambda(1520)}^A}{A \sigma_{\Lambda(1520)}^C}, \quad (17)$$

where $\sigma_{\Lambda(1520)}^A$ and $\sigma_{\Lambda(1520)}^C$ are the inclusive differential (16) or total⁶⁾ cross sections for $\Lambda(1520)$ production in $\pi^- A$ and $\pi^- C$ collisions, respectively.

⁵⁾ Evidently, the first two scenarios for the total $\Lambda(1520)$ in-medium width correspond to the factors $f = 0$ and $f = 1$.

⁶⁾ Obtained by integration of the differential cross sections (16) over $\Lambda(1520)$ momentum.

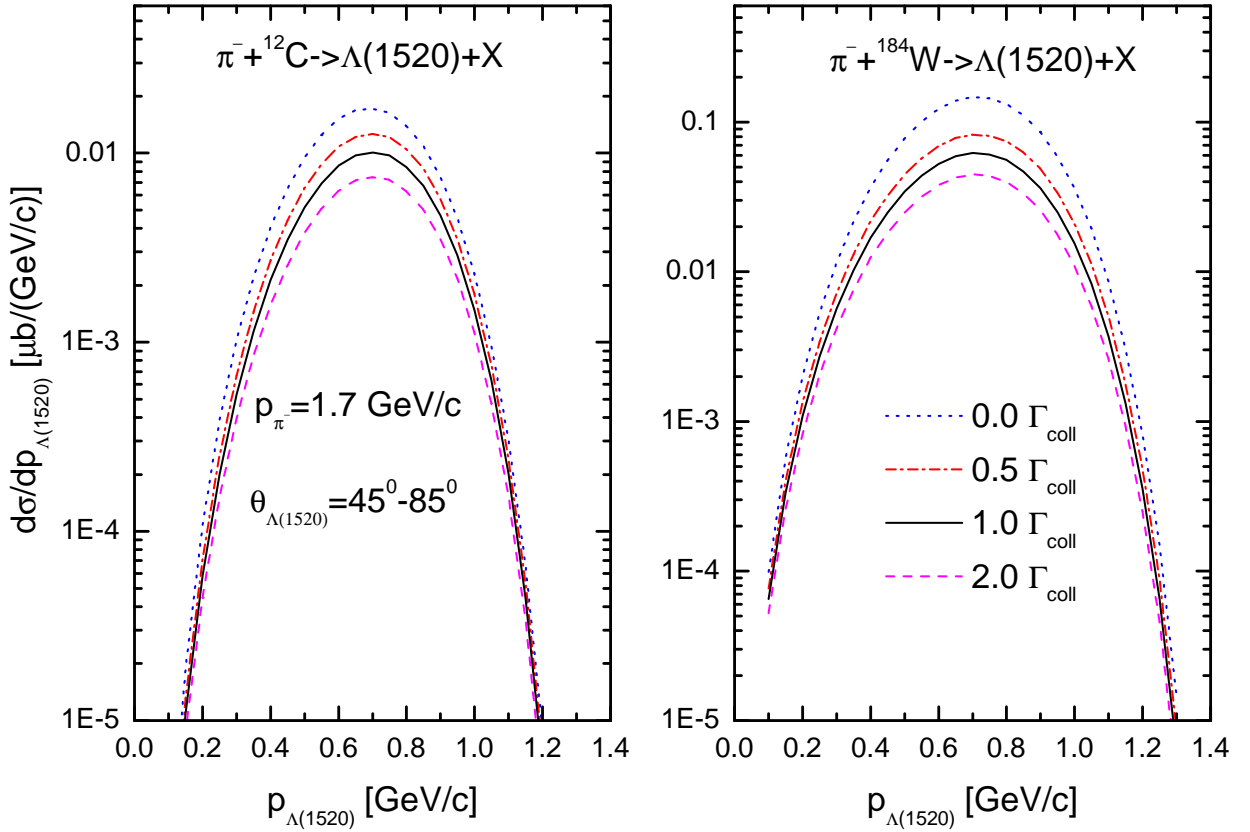


Figure 5: (color online) The same as in Fig.3 but for the laboratory polar angular range of 45° – 85° .

3 Results and discussion

At first, we consider the absolute $\Lambda(1520)$ momentum differential cross sections from the direct process (1) in $\pi^{-12}\text{C}$ and $\pi^{-184}\text{W}$ collisions for an incident pion momentum of 1.7 GeV/c. These cross sections were calculated according to Eq. (16) in four considered scenarios for the total $\Lambda(1520)$ in-medium width (see Fig. 2) at laboratory angles of 10° – 45° , 0° – 10° and 45° – 85° . They are given, respectively, in Figs. 3, 4 and 5. One can see that the $\Lambda(1520)$ hyperons are mainly emitted at laboratory angles $\leq 45^\circ$ belonging to the HADES acceptance window. The absolute values of the differential cross sections have at these angles a well measurable strength ~ 1 – $100 \mu\text{b}/(\text{GeV}/c)$ in the high-momentum region of 0.7 – $1.4 \text{ GeV}/c$. Here there are a sizeable differences, especially for the heavy target nucleus ^{184}W , between the results obtained by using different $\Lambda(1520)$ in-medium widths under consideration. They are ~ 20 – 30% for ^{12}C and ~ 30 – 50% for ^{184}W between all calculations corresponding to different choices for this width.

To see more clearly the sensitivity of the $\Lambda(1520)$ hyperon yield to its in-medium width, we show in Fig. 6 on a linear scale the ratio between the differential cross sections for $\Lambda(1520)$ hyperon production on ^{12}C and ^{184}W nuclei, calculated for different options for its total in-medium width as presented in Figs. 3, 4, and the respective differential cross sections, determined in the scenario where the absorption of $\Lambda(1520)$ hyperons in nuclear matter is governed by their free width. It is seen that there are indeed experimentally distinguishable differences between the considered options for the $\Lambda(1520)$ in-medium width for both target nuclei and for both forward laboratory polar $\Lambda(1520)$

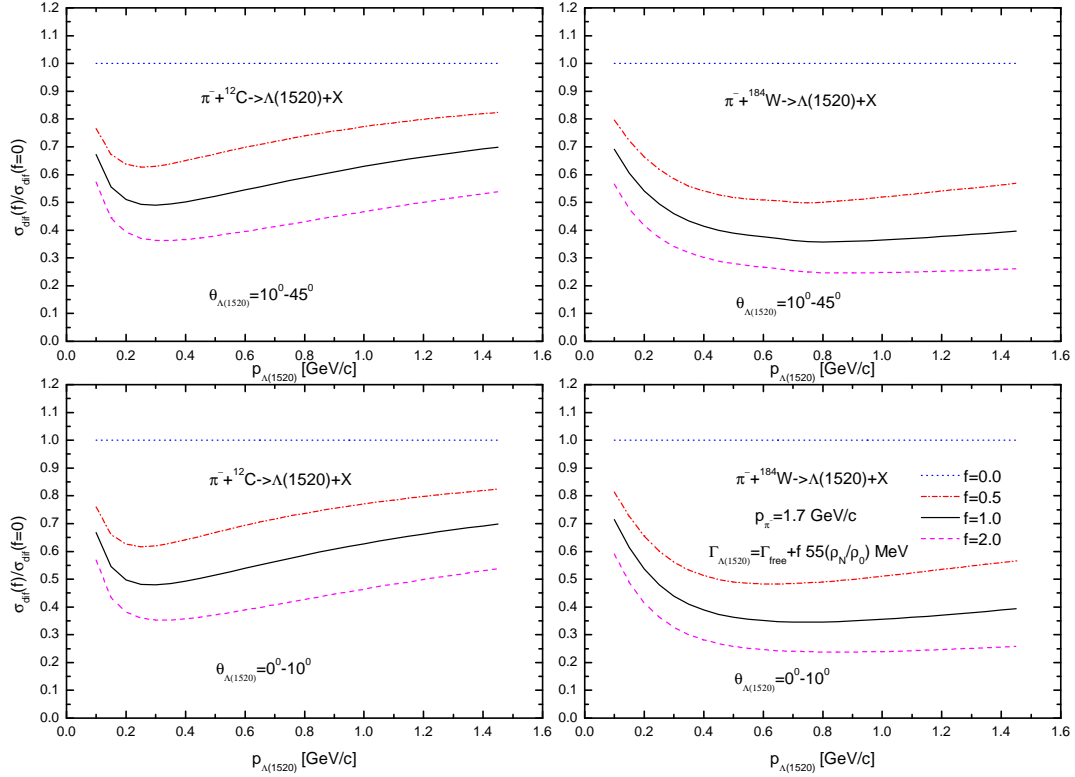


Figure 6: (color online) Ratio between the differential cross sections of $\Lambda(1520)$ production on ^{12}C and ^{184}W target nuclei at laboratory angles of $10^\circ\text{--}45^\circ$ (upper two panels) and $0^\circ\text{--}10^\circ$ (lower two panels) by 1.7 GeV/c π^- mesons in the primary $\pi^-p \rightarrow K^0\Lambda(1520)$ reactions calculated within different scenarios for the total $\Lambda(1520)$ hyperon in-medium width in which its collisional width was multiplied by the factors indicated in the inset, and the same cross sections, obtained in the scenario where the absorption of $\Lambda(1520)$ hyperons in nuclear matter is governed by their free width (dotted curve in Fig. 2), as a function of $\Lambda(1520)$ momentum.

angular domains. Thus, for example, the $\Lambda(1520)$ momentum distributions are reduced at collisional width $0.5\cdot\Gamma_{\text{coll}}$ by factors of about 1.3 and 2.0 as compared to those obtained without this width at momentum of 1.0 GeV/c and laboratory angular range of $0^\circ\text{--}10^\circ$ for ^{12}C and ^{184}W target nuclei, respectively. When going from $0.5\cdot\Gamma_{\text{coll}}$ to $1.0\cdot\Gamma_{\text{coll}}$, the corresponding reduction factors are of about 1.2 and 1.4 at these $\Lambda(1520)$ momentum and angular range; while they are about 1.4 and 1.5 when going from $1.0\cdot\Gamma_{\text{coll}}$ to $2.0\cdot\Gamma_{\text{coll}}$.

We, therefore, come to the conclusion that the in-medium properties of $\Lambda(1520)$ hyperons could be in principle studied at the GSI pion beam facility, using the HADES spectrometer, through the momentum dependence of their absolute production cross sections in π^-A interactions at an initial pion momentum of 1.7 GeV/c.

The sensitivity of the $\Lambda(1520)$ production differential cross sections at laboratory angles $\leq 45^\circ$ in the momentum range $\sim 0.7\text{--}1.4$ GeV/c (where they are largest) to its in-medium width, shown in Figs. 3, 4, can be also studied from such integral measurements as the measurements of the total cross sections for $\Lambda(1520)$ production in $\pi^-^{12}\text{C}$ and $\pi^-^{184}\text{W}$ reactions by 1.7 GeV/c pions in the full-

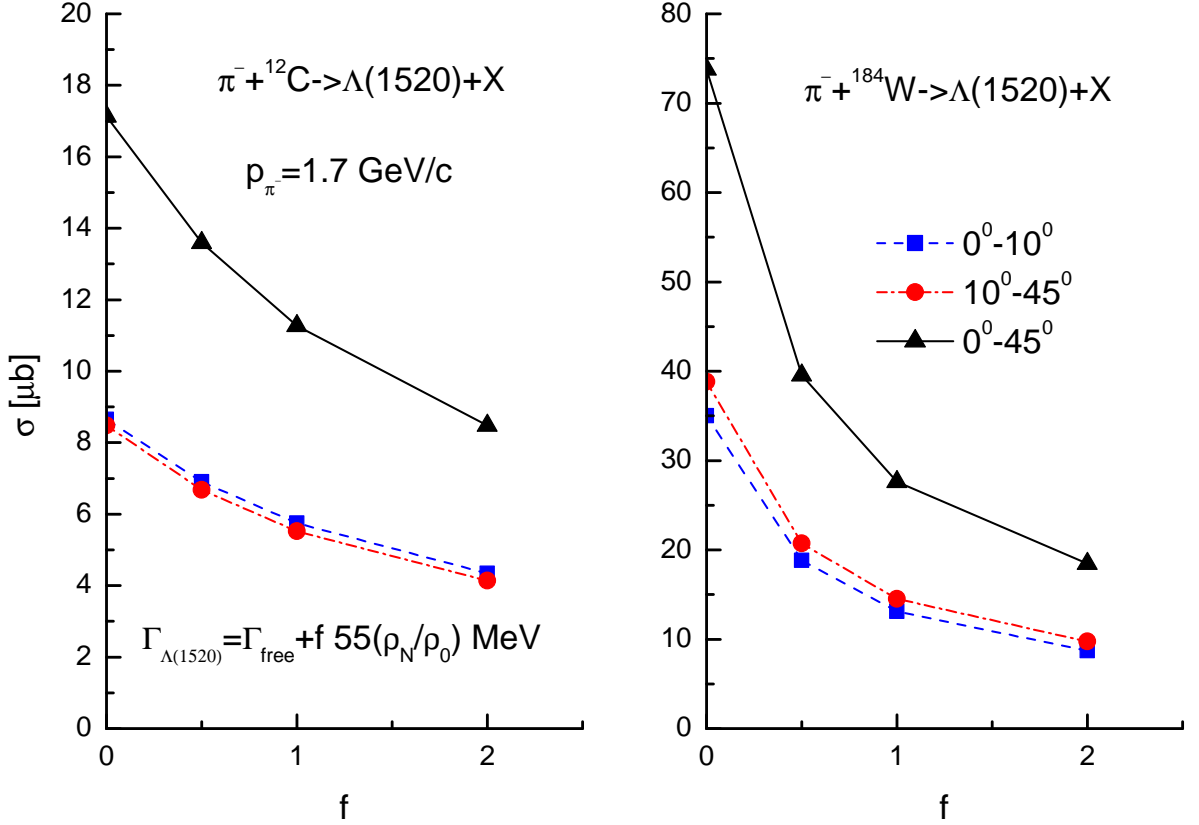


Figure 7: (color online) The total cross sections for the production of $\Lambda(1520)$ hyperons from the primary $\pi^- p \rightarrow K^0 \Lambda(1520)$ channel on ${}^{12}\text{C}$ and ${}^{184}\text{W}$ target nuclei with momenta of 0.1–1.45 GeV/c in the laboratory polar angular ranges of $0^\circ-10^\circ$, $10^\circ-45^\circ$ and $0^\circ-45^\circ$ by 1.7 GeV/c π^- mesons as functions of the factor f by which we multiply their collisional width in our model calculations. The lines are to guide the eye.

momentum region of 0.1–1.45 GeV/c. These cross sections, calculated for the $\Lambda(1520)$ laboratory angular ranges of $0^\circ-10^\circ$, $10^\circ-45^\circ$ and $0^\circ-45^\circ$ by integrating Eq. (16) over the $\Lambda(1520)$ momentum p_{Λ^*} in these ranges, are shown in Fig. 7 as functions of the factor f by which the $\Lambda(1520)$ collisional width [10, 11, 17] was multiplied in our model calculations. One can see that the total cross sections in the angular regions of $0^\circ-10^\circ$ and $10^\circ-45^\circ$ are practically the same for both target nuclei. They, as well as the sum of them (angular domain of $0^\circ-45^\circ$) reveal some sensitivity to the total $\Lambda(1520)$ in-medium width. Thus, the $\Lambda(1520)$ total cross sections in these three angular domains are reduced at collisional width $0.5 \cdot \Gamma_{\text{coll}}$ by factors of about 1.3 and 1.9 as compared to those obtained without this width for ${}^{12}\text{C}$ and ${}^{184}\text{W}$ target nuclei, respectively. When going from $0.5 \cdot \Gamma_{\text{coll}}$ to $1.0 \cdot \Gamma_{\text{coll}}$, the corresponding reduction factors are about 1.2 and 1.4; and they are about 1.3 and 1.5 when going from $1.0 \cdot \Gamma_{\text{coll}}$ to $2.0 \cdot \Gamma_{\text{coll}}$. Therefore, a comparison of the "integral" results, presented in Fig. 7, with the respective experimentally determined total $\Lambda(1520)$ hyperon production cross sections will also allow one to obtain information about its in-medium width.

Fig. 8 shows the momentum dependence of the transparency ratio T_A for the target combination W/C for $\Lambda(1520)$ hyperons produced in the direct reaction channel (1) at laboratory angles of $0^\circ-10^\circ$ and $10^\circ-45^\circ$ by 1.7 GeV/c pions. The transparency ratio is calculated on the basis of Eq. (17)

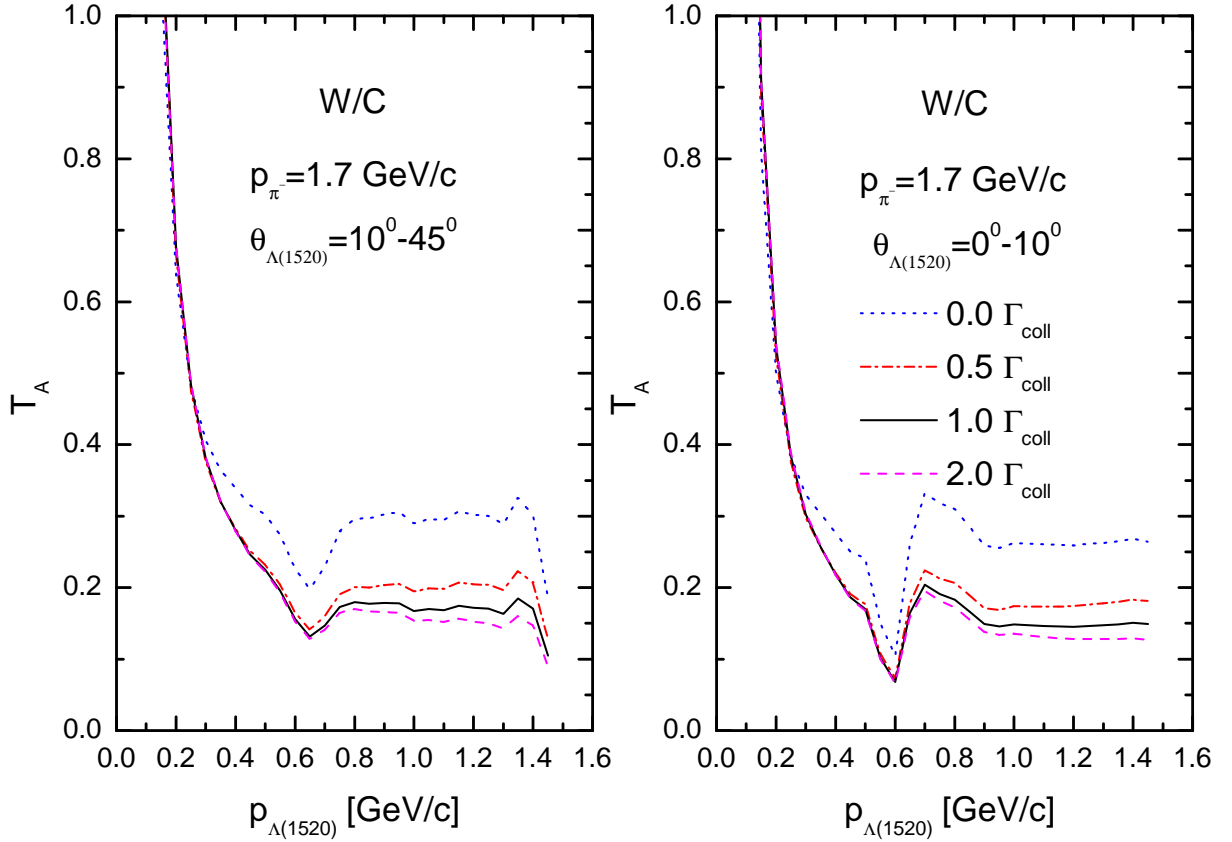


Figure 8: (color online) Transparency ratio T_A as a function of the $\Lambda(1520)$ momentum for combination $^{184}\text{W}/^{12}\text{C}$ as well as for the $\Lambda(1520)$ laboratory polar angular ranges of $10^\circ\text{--}45^\circ$ (left) and $0^\circ\text{--}10^\circ$ (right), for an incident π^- meson momentum of 1.7 GeV/c, calculated within different scenarios for the total $\Lambda(1520)$ hyperon in-medium width where its collisional width is multiplied by the factors indicated in the inset.

using the results obtained for the adopted options of the $\Lambda(1520)$ in-medium width and given in Figs. 3, 4. It is seen from this figure that there are measurable changes $\sim 30\%$ in the quantity T_A only between calculations corresponding to the cases when the loss of $\Lambda(1520)$ hyperons in nuclear matter is determined by their free width and by the sum of this width and collisional width of the type $0.5\cdot\Gamma_{\text{coll}}$ at the momenta of interest $\sim 0.7\text{--}1.4$ GeV/c. On the other hand, the differences between the choices $0.5\cdot\Gamma_{\text{coll}}$ and $1.0\cdot\Gamma_{\text{coll}}$, $1.0\cdot\Gamma_{\text{coll}}$ and $2.0\cdot\Gamma_{\text{coll}}$ for $\Lambda(1520)$ collisional width are almost insignificant. They are $\sim 10\text{--}15\%$. This means that the momentum dependence of the transparency ratio cannot be employed for reliable determination of the $\Lambda(1520)$ in-medium width from the HADES near-threshold $\Lambda(1520)$ production measurements in $\pi^- A$ interactions. The transparency ratio T_A exhibits dips at momenta $\sim 0.6\text{--}0.7$ GeV/c. This can be explained by the fact that the differential cross sections for $\Lambda(1520)$ production on ^{184}W target nucleus "is bent down" at these momenta (see Figs. 3, 4) due to the off-shell kinematics of the first chance $\pi^- p$ collision and the role played by the nucleus-related effects such as the struck target proton binding and Fermi motion, encoded in the nuclear spectral function $P_A(\mathbf{p}_t, E)$. The spectral functions for ^{12}C and ^{184}W , adopted in the calculations, are different [21, 23–25].

In Fig. 9 we show the "integral" transparency ratio T_A for the target combination W/C for

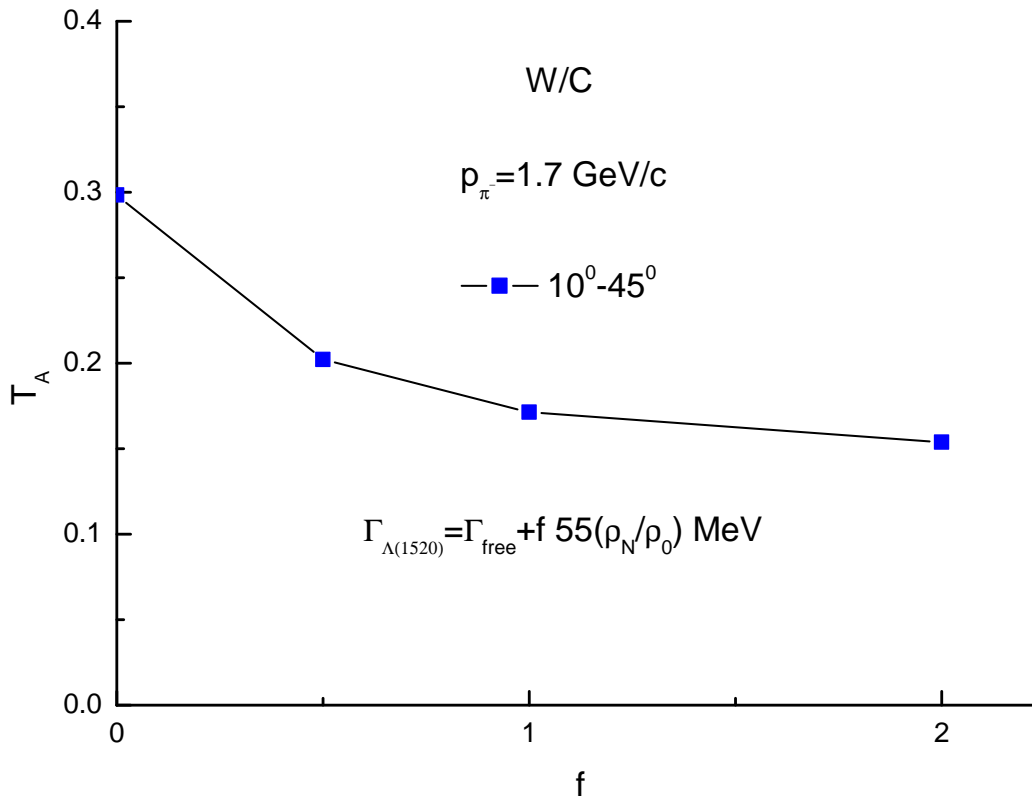


Figure 9: (color online) Transparency ratio T_A for $\Lambda(1520)$ hyperons from primary $\pi^-p \rightarrow K^0\Lambda(1520)$ reactions at incident π^- meson momentum of 1.7 GeV/c for the target combination $^{184}\text{W}/^{12}\text{C}$ as well as for the $\Lambda(1520)$ laboratory polar angular range of $10^\circ\text{--}45^\circ$ and momentum range of 0.1–1.45 GeV/c as a function of the factor f . The line is to guide the eye.

$\Lambda(1520)$ hyperons produced at laboratory angles of $10^\circ\text{--}45^\circ$ and momenta of 0.1–1.45 GeV/c by 1.7 GeV/c pions as a function of the factor f by which their nominal collisional width predicted in [10, 11, 17] is multiplied in our calculations. This "integral" quantity is calculated according to Eq. (17) using the results for the total $\Lambda(1520)$ production cross sections presented in Fig. 7. One can see that the differences between all calculations corresponding to different choices of the $\Lambda(1520)$ in-medium width are similar to those of Fig. 8.

Taking into account the above consideration, we can conclude that the $\Lambda(1520)$ absolute momentum distribution measurements in near-threshold $\pi^-^{12}\text{C}$ and $\pi^-^{184}\text{W}$ reactions might allow one to shed light on the $\Lambda(1520)$ in-medium width. However, its relative yield (both "differential" and "integral") in these reactions cannot serve as reliable tool for determining this width.

4 Conclusions

In the present paper we study the pion-induced inclusive $\Lambda(1520)$ hyperon production from ^{12}C and ^{184}W target nuclei near threshold within a nuclear spectral function approach accounting for incoherent primary π^- meson–proton $\pi^-p \rightarrow K^0\Lambda(1520)$ production processes. We calculate the

absolute differential and total cross sections for production of $\Lambda(1520)$ hyperons off these nuclei at laboratory angles of 0° – 10° , 10° – 45° and 45° – 85° by 1.7 GeV/c π^- mesons as well as their relative (transparency ratio) differential and integral yields for four scenarios of the $\Lambda(1520)$ total in-medium width. We demonstrate that these absolute observables, contrary to the relative ones, reveal some sensitivity to the $\Lambda(1520)$ in-medium width. Therefore, their measurement in a dedicated experiment at the GSI pion beam facility will allow to shed light on this width.

Acknowledgments

The authors would like to thank Volker Metag for careful reading of the manuscript and valuable comments on it.

References

- [1] R. Rapp and J. Wambach, *Adv. Nucl. Phys.* **25**, 1 (2000).
- [2] R. S. Hayano and T. Hatsuda, *Rev. Mod. Phys.* **82**, 2949 (2010).
- [3] S. Leupold, V. Metag, and U. Mosel, *Int. J. Mod. Phys. E***19**, 147 (2010).
- [4] G. Krein, A. W. Thomas, and K. Tsushima, arXiv:1706.02688 [hep-ph].
- [5] V. Metag, M. Nanova, and E. Ya. Paryev, *Prog. Part. Nucl. Phys.* **97**, 199 (2017).
- [6] A. Gal, E. V. Hungerford and D. J. Millener, *Rev. Mod. Phys.* **88**, 035004 (2016).
- [7] K. Tsushima *et al.*, *Phys. Rev. C* **83**, 065208 (2011);
G. Krein, A. W. Thomas, and K. Tsushima, *Phys. Lett. B* **697**, 136 (2011).
- [8] E. Ya. Paryev, Yu. T. Kiselev, and Yu. M. Zaitsev, *Nucl. Phys. A* **968**, 1 (2017);
E. Ya. Paryev and Yu. T. Kiselev, *Nucl. Phys. A* **978**, 201 (2018);
E. Ya. Paryev and Yu. T. Kiselev, *Phys. Atom. Nucl. Vol.* **80**, No.1, 67 (2017);
E. Ya. Paryev and Yu. T. Kiselev, *Phys. Atom. Nucl. Vol.* **81**, No.5, 566 (2018);
E. Ya. Paryev, *Nucl. Phys. A* **988**, 24 (2019).
- [9] S. D. Bass and P. Moskal, arXiv:1810.12290 [hep-ph].
- [10] M. M. Kaskulov and E. Oset, *Phys. Rev. C* **73**, 045213 (2006).
- [11] M. M. Kaskulov and E. Oset, *AIP Conf. Proc.* **842**, 483–5 (2006).
- [12] M. F. M. Lutz, C. L. Copra and M. Moeller, *Nucl. Phys. A* **808**, 124 (2008).
- [13] D. Cabrera *et al.*, *Phys. Rev. C* **90**, 055207 (2014).
- [14] S. Petschauer *et al.*, *Eur. Phys. J. A* **52**, 15 (2016).
- [15] E. Ya. Paryev, M. Hartmann, and Yu. T. Kiselev, *Chinese Physics C*,
Vol. **41**, No. (12), 124108 (2017).
- [16] Z. Q. Feng, W. J. Xie, and G. M. Jin, *Phys. Rev. C* **90**, 064604 (2014).

- [17] M. Kaskulov, L. Roca and E. Oset, *Eur. Phys. J. A* **28**, 139 (2006).
- [18] E. Ya. Paryev, *Phys. Atom. Nucl. Vol.* **75**, No.12, 1523 (2012).
- [19] E. Ya. Paryev, *J. Phys. G: Nucl. Part. Phys.* **37**, 105101 (2010).
- [20] J. Adamczewski-Musch *et al.* (HADES Collaboration), *Phys. Rev. Lett.* **123**, 022002 (2019).
- [21] E. Ya. Paryev, *Chinese Physics C*, Vol. **42**, No. (8), 084101 (2018).
- [22] J. A. Kadyk *et al.*, *Nucl. Phys. B* **27**, 13 (1971);
J. M. Hauptman, J. A. Kadyk, and G. H. Trilling, *Nucl. Phys. B* **125**, 29 (1977).
- [23] S. V. Efremov and E. Ya. Paryev, *Eur. Phys. J. A* **1**, 99 (1998).
- [24] E. Ya. Paryev, *Eur. Phys. J. A* **9**, 521 (2000).
- [25] E. Ya. Paryev, *Eur. Phys. J. A* **7**, 127 (2000).
- [26] A. Baldini *et al.*, in *Total Cross Sections of High Energy Particles*, edited by H. Schopper, Landolt-Börnstein, New Series, Vol. I/12a, Springer-Verlag, Berlin (1988).